Computational Chemistry Hot Paper

How to cite: *Angew. Chem. Int. Ed.* **2021**, *60*, 8700–8704
International Edition: doi.org/10.1002/anie.202100940
German Edition: doi.org/10.1002/ange.202100940

Planar Hexacoordinate Carbons: Half Covalent, Half Ionic

Luis Leyva-Parra, Luz Diego, Osvaldo Yañez, Diego Inostroza, Jorge Barroso, Alejandro Vásquez-Espinal,* Gabriel Merino,* and William Tiznado**

Abstract: *Herein, the first global minima containing a planar hexacoordinate carbon (phC) atom are reported. The fifteen structures belong to the $CE_3M_3^+$ (E = S–Te and M = Li–Cs) series and satisfy both geometric and electronic criteria to be considered as a true phC. The design strategy consisted of replacing oxygen in the D_{3h} $CO_3Li_3^+$ structure with heavy and less electronegative chalcogens, inducing a negative charge on the C atom and an attractive electrostatic interaction between C and the alkali-metal cations. The chemical bonding analyses indicate that carbon is covalently bonded to three chalcogens and ionically connected to the three alkali metals.*

In 1970, Hoffmann and co-workers stated that incorporating π-acceptor/σ-donor ligands could stabilize a transition state with a planar tetracoordinate carbon (ptC).[1] The approach was successfully adopted by the group of Schleyer to predict the first local minimum with this peculiar form.[2] In 1977, the complex V_2(2,6-dimethoxyphenyl)$_4$ was characterized via X-ray diffraction.[3] Although, for more than two years the presence of two ptCs in this complex remained unnoticed.[4] These findings inspired the design of more ptCs, and later extended to explore for penta- and hexacoordinate carbon species.[5–11] However, the more the coordination number increases, the more elusive these species become. So far, only a handful of global minima structures with a planar penta-coordinate carbon (ppC) are known,[6,12] and not a single planar hexacoordinate carbon (phC). Note that the reported CBe_2 monolayer is the most stable layer with a quasi-planar hexacoordinate carbon moiety.[13]

The D_{6h} CB_6^{2-} cluster (**1**) was the first phC candidate,[14] but it is 143.9 kJ mol^{-1} higher in energy than its most stable isomer.[15] Although **1** is only a local minimum, this cluster was used as a framework by Wu et al.[16] to design, via an isoelectronic substitution, two additional phC candidates with D_{3h} symmetry, $CN_3Be_3^+$ and $CO_3Li_3^+$ (**2** and **3** in Figure 1). The authors located **2** at 25.5 kJ mol^{-1} above the lowest-lying energy form and **3** as the putative global minimum.

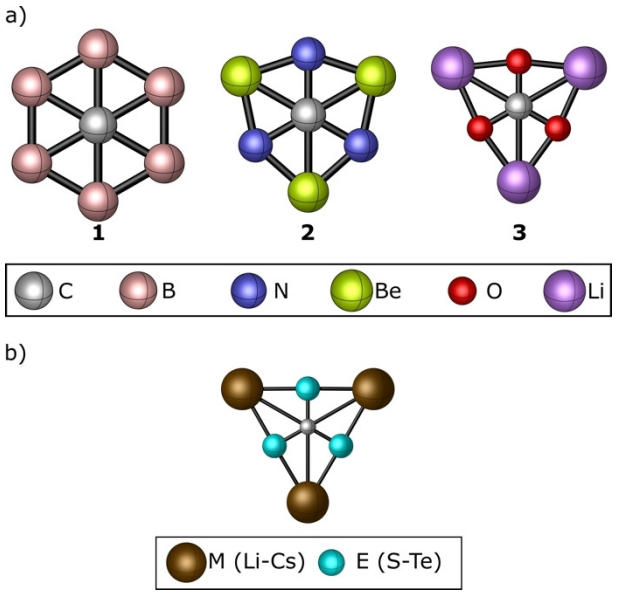

Figure 1. D_{3h} structures of a) CB_6^{2-}, $CN_3Be_3^+$, and $CO_3Li_3^+$; b) The global minima of the $CE_3M_3^+$ (E = S–Te and M = Li–Cs) series.

According to the authors, the carbonate dianion CO_3^{2-} is electrostatically stabilized by the three bridging Li^+ counterions in **3**. Since the C–Li contacts are shorter than the C–Li distances in the methyllithium tetramer and hexamer (2.31 Å),[17] carbon "touches" the surrounding six atoms, i.e., the hexacoordination was assumed based only on a geometrical criterion. IUPAC defines the coordination number of a specified atom in a chemical species as "the number of other atoms directly linked to that specified atom".[18] So, the question remaining is whether the C is truly hexacoordinate. Our computations indicate positive natural charges on C and Li atoms in **3** ($q_c = +0.87\,|e|$ and $q_{Li} = +0.97\,|e|$), implying

[*] L. Leyva-Parra, Dr. O. Yañez, D. Inostroza, Dr. A. Vásquez-Espinal, Prof. W. Tiznado
Computational and Theoretical Chemistry Group
Departamento de Ciencias Químicas
Facultad de Ciencias Exactas
Universidad Andres Bello
República 498, Santiago (Chile)
E-mail: a.vasquezespinal@uandresbello.edu
wtiznado@unab.cl

L. Diego
Escuela Profesional de Química
Facultad de Ciencias Naturales
Universidad Nacional Federico Villarreal
Jr. Río Chepén 290, El Agustino, Lima (Perú)

Dr. O. Yañez
Center of New Drugs for Hypertension (CENDHY)
Santiago (Chile)

J. Barroso, Prof. G. Merino
Departamento de Física Aplicada
Centro de Investigación y de Estudios Avanzados, Unidad Mérida
km. 6 Antigua carretera a Progreso
Apdo. Postal 73, Cordemex, Mérida, Yuc. (México)
E-mail: jorge.barroso@cinvestav.mx
gmerino@cinvestav.mx

Supporting information and the ORCID identification number(s) for the author(s) of this article can be found under: https://doi.org/10.1002/anie.202100940.

electrostatic repulsion between them. The interacting quantum atoms[19–22] (IQA) analysis supports a strong repulsion between carbon and lithium (1356.4 kJ mol^{-1}), mostly pure coulombic repulsion (1358.2 kJ mol^{-1}, see Table S1 in the Supporting Information). Indeed, the positive charge on C is expected due to the electronegativity difference between C and O ($\Delta\chi = 1.0$, Scheme 1). How can charges be tuned to facilitate electrostatic interactions between carbon and the alkali metals? Our proposal is to replace oxygen with heavier (and less electronegative) chalcogens in **3**, stabilizing a true planar hexacoordinate carbon atom (Scheme 1, right). The fifteen possible $CE_3M_3^+$ (E = S–Te and M = Li–Cs) combinations satisfy the geometric and electronic criteria to be classified as phC. Remarkably, the phCs here introduced have as a basis well-known reagents, such as CS_3^{2-}, CSe_3^{2-}, and CS_3Na_2,[23–25] implying that their experimental realization is feasible.

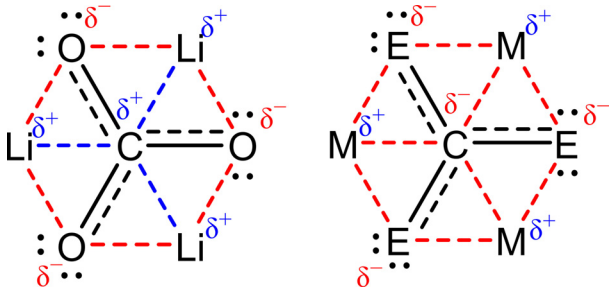

Scheme 1. Schematic hybrid structures of the CO_3^{2-} (left) and hypothetical CE_3^{2-} (right) moieties stabilized by Li^+ and heavier alkali-metal cations (M = Na–Cs), respectively. Red and blue dotted lines represent attractive and repulsive electrostatic interactions, respectively.

A systematic exploration of the potential energy surfaces was carried out using the AUTOMATON[26] and GLOMOS[27] programs. The initial screening in the singlet and triplet states was done at the PBE0[28]-D3[29]/SDD[30,31] level. The low-lying energy isomers (< 125.5 kJ mol^{-1} above the putative global minimum) were reminimized at the PBE0-D3/def2-TZVP[32] level, and relative energies were computed at the CCSD(T)[33,34]/def2-TZVP//PBE0-D3/def2-TZVP level. So, for the energetic discussion, only the latter level is considered. The diagnostic of the T_1 coupled-cluster operator was performed to verify whether the converged CCSD wave functions are based on a single-reference method.[35] All the T_1 values are lower than the suggested threshold of 0.02 (Table S1). The PBE0 and CCSD(T) computations were done using Gaussian 16.[36]

The bonding was analyzed in terms of the Wiberg bond index (WBI)[37] and natural population analysis (NPA),[38] as implemented in the NBO 6.0 program.[39] Additionally, the Adaptive Natural Density Partitioning (AdNDP) method was performed with the Multiwfn program.[40,41] AdNDP recovers the electron-pair Lewis concept as the fundamental chemical bonding component, localizing the *n*-center-two-electron bonds (*nc*-2e). Additionally, IQA[19–22] was used to decompose the interaction energy. IQA rises from a competition between atomic deformation and the additive interatomic interaction energies. The former is an analogue of the classical promotion energy necessary for one atom to bond to another. The latter is composed of classical (or ionic-type) and exchange-correlation (or covalent-type) components. So, the interatomic interaction energy, V_{int}, is the sum of the coulombic, V_C, and exchange-correlation, V_{XC}, terms, where V_C is the exact electrostatic interaction between the electrons and nuclei contained in a pair of basins and includes all the classical electrostatic terms (nuclear repulsion, electron–nucleus attraction, and the Coulomb part of the electron–electron repulsion). The term V_{XC} is purely quantum mechanical in nature, depending only on the exchange-correlation part of the electron–electron interaction. Usually, V_C is related to the ionic-type component of a given interaction, and V_{XC} to electron-sharing or covalent-type interaction. The IQA analysis was performed at the PBE0-D3/Def2TZVP level using the AIMAll program.[42]

All the global minima of the $CE_3M_3^+$ (E = O–Te and M = Li–Cs) clusters adopt a planar D_{3h} symmetry with C–E distances between a single and a double bond (Table 1). This

Table 1: Bond lengths (*r*, Å), charges (*q*, |e|), Wiberg bond indices (WBI), HOMO–LUMO gap (ΔE_{H-L}, eV), and the lowest harmonic vibrational frequency (ν_{min}, cm^{-1}) of the $CE_3M_3^+$ (E = O–Te and M = Li–Cs) computed at the PBE0-D3/def2-TZVP level.[a]

System	r_{C-Ch}	r_{C-M}	r_{Ch-M}	q(C)	q(E)	q(M)	WBI_{C-E}	WBI_{E-M}	ΔE_{H-L}	ν_{min}
$CO_3Li_3^+$	1.28	2.18	1.90	0.87	−0.92	0.97	1.29	0.02	8.34	178
$CO_3Na_3^+$	1.29	2.55	2.21	0.90	−0.94	0.97	1.29	0.02	6.21	103
$CO_3K_3^+$	1.29	2.92	2.54	0.91	−0.94	0.97	1.28	0.02	5.51	75
$CO_3Rb_3^+$	1.29	3.10	2.69	0.91	−0.95	0.98	1.28	0.02	5.05	63
$CO_3Cs_3^+$	1.29	3.22	2.81	0.92	−0.94	0.97	1.28	0.03	5.32	50
$CS_3Li_3^+$	1.71	2.67	2.34	−0.52	−0.41	0.92	1.34	0.07	5.06	54
$CS_3Na_3^+$	1.72	3.08	2.68	−0.51	−0.42	0.93	1.34	0.06	4.72	47
$CS_3K_3^+$	1.72	3.51	3.04	−0.49	−0.45	0.95	1.33	0.04	4.48	37
$CS_3Rb_3^+$	1.72	3.70	3.21	−0.49	−0.45	0.95	1.33	0.04	4.37	30
$CS_3Cs_3^+$	1.72	3.84	3.34	−0.49	−0.45	0.95	1.33	0.04	4.37	26
$CSe_3Li_3^+$	1.86	2.81	2.48	−0.71	−0.33	0.90	1.31	0.08	4.36	−30
$CSe_3Na_3^+$	1.86	3.23	2.81	−0.70	−0.35	0.91	1.31	0.07	4.19	32
$CSe_3K_3^+$	1.86	3.67	3.18	−0.68	−0.38	0.94	1.31	0.05	3.97	24
$CSe_3Rb_3^+$	1.86	3.87	3.36	−0.68	−0.38	0.95	1.31	0.05	3.87	19
$CSe_3Cs_3^+$	1.86	4.03	3.49	−0.68	−0.39	0.95	1.31	0.05	3.86	14
$CTe_3Li_3^+$	2.07	3.04	2.69	−1.03	−0.19	0.87	1.25	0.11	3.45	−54
$CTe_3Na_3^+$	2.07	3.47	3.02	−1.02	−0.21	0.89	1.25	0.10	3.43	22
$CTe_3K_3^+$	2.07	3.92	3.40	−1.01	−0.26	0.93	1.25	0.06	3.26	18
$CTe_3Rb_3^+$	2.07	4.12	3.57	−1.01	−0.26	0.93	1.25	0.06	3.16	14
$CTe_3Cs_3^+$	2.07	4.29	3.72	−1.01	−0.26	0.93	1.25	0.06	3.15	11

[a] The sums of Pyykkö's single-bond radii for the C–Li, C–Na, C–K, C–Rb, and C–Cs bonds are 2.08, 2.30, 2.71, 2.85, and 3.07 Å, respectively.[43] The sums of van der Waals radii for the C–Li, C–Na, C–K, C–Rb, and C–Cs bonds are 3.82, 4.20, 4.43, 4.91, and 5.18 Å, respectively.[44]

is consistent with the corresponding WBI values (1.25–1.34), which estimates the bond order from the natural population analysis. Table 1 shows that the C–M distances are longer than the expected single bond[43] but shorter than the sum of their van der Waals radii. So, it could be considered that in these clusters, carbon "touches" the six surrounding atoms. That is, all of them contain a phC that satisfies the geometrical criteria, as suggested by Wu et al.[16]

Remarkably, the fifteen global minima of the $CE_3M_3^+$ (E = S–Te and M = Li–Cs) series are D_{3h} structures with a phC. It should be mentioned that for $CSe_3Li_3^+$ and $CTe_3Li_3^+$, the D_{3h} isomers show a small imaginary frequency (−30 and −50 cm^{-1}, respectively) corresponding to a slight displacement of carbon from the molecular plane and leading to a C_{3v} global minimum. However, the energy difference between the D_{3h} and C_{3v} arrangements is negligible in both stoichiometries. So, the averaged vibrational mode results in phCs. The corresponding Cartesian coordinates are included in the supplementary information, and other low-lying isomers are listed in Figures S1–S13. With the exception of the cases mentioned above, the smallest vibrational frequencies for the remaining global minima are reasonably large (10–178 cm^{-1}), the singlet state is the most favorable one (the energy difference with the closest triplet ranges from 79.5 to 494.1 kJ mol^{-1}), and the HOMO–LUMO gaps are relatively high, varying between 3.15 and 8.34 eV (Table 1).

NPA charges support that the CE_3 moiety is a dianion electrostatically stabilized by three alkali-metal cations. Besides, the low WBI values (0.02–0.10) of the peripheral E–M might indicate an electrostatic interaction, which is relevant because ligand–ligand contacts contribute significantly to the stabilization of planar hypercoordinate species. Note that the lowest E–M WBIs occur in systems with oxygen. However, the C–M WBI values are zero, and it is not clear if there is an electrostatic interaction or any interaction at all between the center and the alkali metals. On the other hand, in the clusters with heavier chalcogens, contrary to $CO_3M_3^+$ systems, the charge on the carbon atom is negative, suggesting a probable electrostatic interaction with the alkali-metal cation. The negative charge on C increases as the electronegativity of the chalcogen decreases (q(C) is approximately −0.5, −0.7, and −1.0 |e| for S, Se, and Te, respectively), while the charge on the alkali-metal cations has no significant variation. So, the zero C-M WBI values might be the consequence of a pure electrostatic interaction without any orbital overlap involved.

The charge analysis and bond orders are in line with the picture obtained from the AdNDP analysis. Let us analyze $CSe_3K_3^+$ as a representative case. The AdNDP recovers three 2c-2e C–Se σ-bonds and three delocalized π-bonds spread on the CSe_3 moiety. Table S3 shows an identical bonding pattern to $CSe_3K_3^+$ in the other $CE_3M_3^+$ systems. This analysis suggests, once more, that if there is any interaction between CE_3 and the cations, it would be purely electrostatic. A different situation occurs in CB_6^{2-}. Its covalent character is corroborated by the WBI values and the AdNDP analysis (Figure 2). There is a set of six peripheral 2c-2e B–B σ-bonds, with an occupation number (ON) of 1.95 |e|. For this cluster, the C–B and B–B bonds (1.59 Å) are shorter than the corresponding single bond according to the covalent radius of Pyykkö.[43] Most importantly, there are multicenter bonds between C and B, justifying the carbon hypercoordination. In summary, tools like WBI or AdNDP, designed to understand chemical interactions between atoms with orbital overlap such as C–E, cannot confirm whether the carbon and the alkali metals are connected. Nonetheless, the charge analysis points to a possible electrostatic interaction between C and M atoms for E = S, Se, and Te.

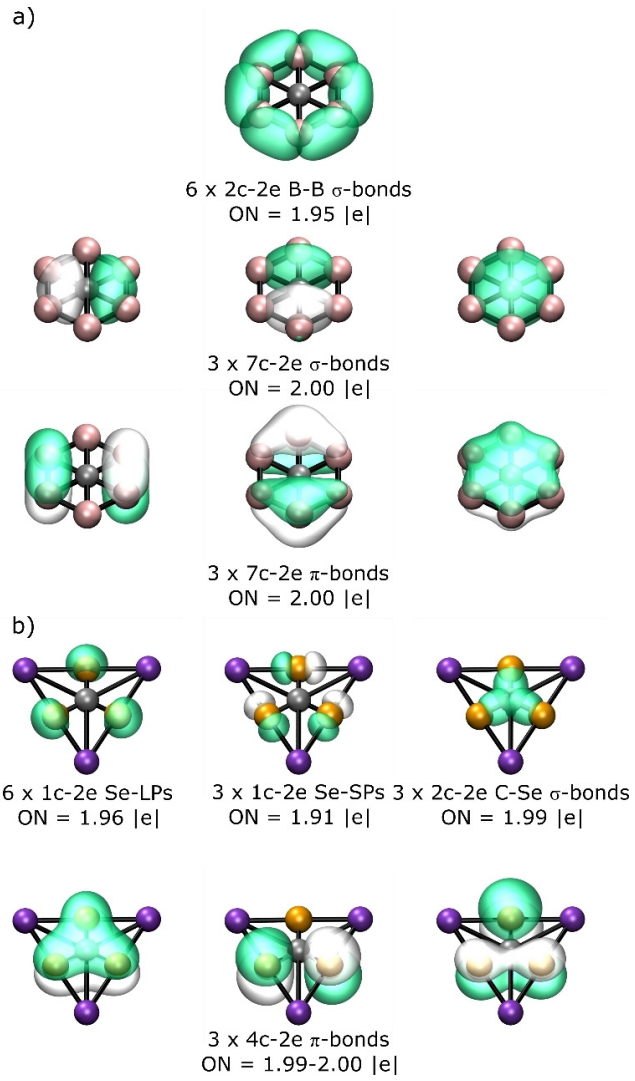

Figure 2. AdNDP analysis of a) CB_6^{2-} and b) $CSe_3K_3^+$. ON stands for occupation number. Carbon = gray, boron = pink, potassium = purple, selenium = orange.

Hence, it is mandatory to use a proper methodology to describe ionic interactions. IQA is an option, offering a more accurate description of such types of interactions. Quite recently, this methodology was fundamental to provide clues to explain the chemical bond in $NaBH_3^-$.[45] The IQA analysis for the CE_3Na^+ series is shown in Table 2. At first sight, $CO_3Na_3^+$ is easily distinguishable from the rest. The IQA interaction energy, V_{IQA}^{Int}, between carbon and oxygen is more than four times greater (−4143.3 kJ mol^{-1}) than with any other remaining chalcogen. The same is true for the

Table 2: Energy components of IQA for the D_{3h} $CE_3Na_3^+$ systems (E = O, S, Se, and Te); V_{IQA}^{int}, V_C^{int}, and V_{XC}^{int} are the interatomic IQA interaction energy and their coulombic and exchange-correlation energy components, respectively, in kJ mol^{-1}.

	$CO_3Na_3^+$	$CS_3Na_3^+$	$CSe_3Na_3^+$	$CTe_3Na_3^+$
V_{IQA}^{int}(C–E)	−4143.3	−981.5	−901.7	−911.1
V_C^{int}(C–E)	−3358.5	−12.4	−37.7	−164.4
V_{XC}^{int}(C–E)	−784.7	−969.1	−864.0	−746.7
V_{IQA}^{int}(C–Na)	**1148.4**	**−234.0**	**−264.0**	**−393.3**
V_C^{int}(C–Na)	**1150.2**	**−231.0**	**−261.0**	**−336.6**
V_{XC}^{int}(C–Na)	**−1.8**	**−3.2**	**−3.0**	**−2.7**
V_{IQA}^{int}(E–Na)	−839.6	−244.4	−213.1	−160.4
V_C^{int}(E–Na)	−780.6	−191.5	−161.8	−110.2
V_{XC}^{int}(E–Na)	−59.1	−52.8	−51.3	−50.2

alkali-metal interaction, which is three to five times larger with oxygen (−839.6 kJ mol^{-1}). These strong C–O and O–Na stabilizing interactions occur at the expense of a strong repulsion of the center with the alkali metal (1148.4 kJ mol^{-1}). This is in perfect agreement with the previous analyses. The higher interaction of carbon and oxygen exceeds the repulsion with sodium, forming a CO_3^{2-} fragment bridged by alkali metals attracted to the oxygens.

Now, let us analyze the rest of the systems in the series. The IQA interaction energy between the C and each E is the major attractive component. The value decreases in magnitude with heavier chalcogens (from −981.5 to −901.7 kJ mol^{-1}). The interactions between peripheral atoms, E–Na, essential for the stabilization of the system, have similar decreasing behavior (from −244.4 to −160.4 kJ mol^{-1}). In contrast, the C–Na interaction energy increases from S to Te (from −234.0 to −393.3 kJ mol^{-1}). Above all, these structures show an electrostatic attraction between carbon and sodium, essentially coulombic (approximately 99%). These results are in total agreement with the charge analysis. The decrease of the chalcogen's electronegativity leads to an increase in carbon's negative charge, which will enforce the electrostatic interaction with the sodium cation. This electrostatic interaction between C and M is found in all the global minima of the $CE_3M_3^+$ (E = S–Te and M = Li–Cs) series, as shown in Tables S4–S7. In other words, all the bonding analyses clearly support that carbon atoms are covalently bonded to the chalcogens and electrostatically to the alkali metals, so these species contain a truly hexacoordinate carbon atom.

Roald Hoffmann stated: "…the purpose of studying nonclassical molecules is to learn from the abnormal… the making of molecules that are untypical or abnormal test our understanding of that fundamental yet fussy entity -the chemical bond".[46] What is more abnormal than a phC? Introducing the first global minima containing a phC is therefore per se relevant for chemistry. The fifteen global minima of the $CE_3M_3^+$ (E = S–Te and M = Li–Cs) series contrast with the reported $CO_3Li_3^+$ because the substitution of oxygen by heavier group 16 elements induces a charge transfer from the chalcogen to carbon, leading to electrostatic interactions with the alkali metals. The bonding analysis confirms that carbon forms covalent bonds with the chalcogens and attractive electrostatic interactions with the alkali metals. These systems satisfy both geometric and electronic criteria to be considered as true planar hexacoordinate carbon atoms and, most importantly, some of the CE_3^{2-} frameworks are experimentally known reagents, making the phC detection feasible.

Acknowledgements

The authors are grateful for the financial support of the grants: National Agency for Research and Development (ANID)/Scholarship Program/BECAS DOCTORADO NACIONAL/2019–21190427. National Agency for Research and Development (ANID)/Scholarship Program/BECAS DOCTORADO NACIONAL/2020-21201177 and Fondecyt grant 1181165. Powered@NLHPC: This research was partially supported by the supercomputing infrastructure of the NLHPC (ECM-02). The work in Mexico is supported by Grant SEP-Cinvestav-2018-57. J.B. thanks Conacyt for his PhD fellowship.

Conflict of interest

The authors declare no conflict of interest.

Keywords: Hypercoordination · Hypervalence · Planar hexacoordinate carbon · Planar tetracoordinate carbon

[1] R. Hoffmann, R. W. Alder, C. F. Wilcox, *J. Am. Chem. Soc.* **1970**, *92*, 4992–4993.
[2] J. B. Collins, J. D. Dill, E. D. Jemmis, Y. Apeloig, P. v. R. Schleyer, R. Seeger, J. A. Pople, *J. Am. Chem. Soc.* **1976**, *98*, 5419–5427.
[3] F. A. Cotton, M. Millar, *J. Am. Chem. Soc.* **1977**, *99*, 7886–7891.
[4] R. Keese, A. Pfenninger, A. Roesle, *Helv. Chim. Acta* **1979**, *62*, 326–334.
[5] Z.-X. Wang, P. v. R. Schleyer, *Science* **2001**, *292*, 2465–2469.
[6] V. Vassilev-Galindo, S. Pan, K. J. Donald, G. Merino, *Nat. Rev. Chem.* **2018**, *2*, 114.
[7] R. Grande-Aztatzi, J. L. Cabellos, R. Islas, I. Infante, J. M. Mercero, A. Restrepo, G. Merino, *Phys. Chem. Chem. Phys.* **2015**, *17*, 4620–4624.
[8] Y. Pei, W. An, K. Ito, P. v. R. Schleyer, X. C. Zeng, *J. Am. Chem. Soc.* **2008**, *130*, 10394–10400.
[9] Y. Wang, F. Li, Y. Li, Z. Chen, *Nat. Commun.* **2016**, *7*, 11488.
[10] Z.-h. Cui, V. Vassilev-Galindo, J. L. Cabellos, E. Osorio, M. Orozco, S. Pan, Y.-h. Ding, G. Merino, *Chem. Commun.* **2017**, *53*, 138–141.
[11] S. Pan, J. L. Cabellos, M. Orozco-Ic, P. K. Chattaraj, L. Zhao, G. Merino, *Phys. Chem. Chem. Phys.* **2018**, *20*, 12350–12355.
[12] J.-C. Guo, L.-Y. Feng, J. Barroso, G. Merino, H.-J. Zhai, *Chem. Commun.* **2020**, *56*, 8305–8308.
[13] Y. Li, Y. Liao, Z. Chen, *Angew. Chem. Int. Ed.* **2014**, *53*, 7248–7252; *Angew. Chem.* **2014**, *126*, 7376–7380.
[14] K. Exner, P. v. R. Schleyer, *Science* **2000**, *290*, 1937–1940.
[15] B. B. Averkiev, D. Y. Zubarev, L. M. Wang, W. Huang, L.-S. Wang, A. I. Boldyrev, *J. Am. Chem. Soc.* **2008**, *130*, 9248–9250.
[16] Y.-B. Wu, Y. Duan, G. Lu, H.-G. Lu, P. Yang, P. v. R. Schleyer, G. Merino, R. Islas, Z.-X. Wang, *Phys. Chem. Chem. Phys.* **2012**, *14*, 14760–14763.

[17] W. N. Setzer, P. v. R. Schleyer, *Adv. Organomet. Chem.* **1985**, *24*, 353 – 451.
[18] P. Muller, *Pure Appl. Chem.* **1994**, *66*, 1077 – 1184.
[19] A. M. Pendás, M. A. Blanco, E. Francisco, *J. Chem. Phys.* **2004**, *120*, 4581 – 4592.
[20] A. M. Pendás, E. Francisco, M. A. Blanco, *J. Comput. Chem.* **2005**, *26*, 344 – 351.
[21] M. A. Blanco, A. M. Pendás, E. Francisco, *J. Chem. Theory Comput.* **2005**, *1*, 1096 – 1109.
[22] A. M. Pendás, M. A. Blanco, E. Francisco, *J. Comput. Chem.* **2007**, *28*, 161 – 184.
[23] S. M. Aucott, C. J. Burchell, A. M. Z. Slawin, J. D. Woollins, *Phosphorus Sulfur Silicon Relat. Elem.* **2004**, *179*, 903 – 906.
[24] C. J. Burchell, S. M. Aucott, A. M. Z. Slawin, J. D. Woollins, *Dalton Trans.* **2005**, *4*, 735 – 739.
[25] M. Kazemi, L. Shiri, H. Kohzadi, *Phosphorus Sulfur Silicon Relat. Elem.* **2015**, *190*, 1398 – 1409.
[26] O. Yañez, R. Báez-Grez, D. Inostroza, W. A. Rabanal-León, R. Pino Rios, J. Garza, W. Tiznado, *J. Chem. Theory Comput.* **2019**, *15*, 1463 – 1475.
[27] R. Grande-Aztatzi, P. R. Martínez-Alanis, J. L. Cabellos, E. Osorio, A. Martínez, G. Merino, *J. Comput. Chem.* **2014**, *35*, 2288 – 2296.
[28] C. Adamo, V. Barone, *J. Chem. Phys.* **1999**, *110*, 6158 – 6170.
[29] S. Grimme, J. Antony, S. Ehrlich, H. Krieg, *J. Chem. Phys.* **2010**, *132*, 154104.
[30] P. Fuentealba, L. Von Szentpaly, H. Preuss, H. Stoll, *J. Phys. B* **1985**, *18*, 1287.
[31] A. Bergner, M. Dolg, W. Küchle, H. Stoll, H. Preuss, *Mol. Phys.* **1993**, *80*, 1431 – 1441.
[32] F. Weigend, R. Ahlrichs, *Phys. Chem. Chem. Phys.* **2005**, *7*, 3297 – 3305.
[33] R. J. Bartlett, M. Musiał, *Rev. Mod. Phys.* **2007**, *79*, 291.
[34] K. Raghavachari, G. W. Trucks, J. A. Pople, M. Head-Gordon, *Chem. Phys. Lett.* **1989**, *157*, 479 – 483.
[35] T. J. Lee, P. R. Taylor, *Int. J. Quantum Chem.* **1989**, *36*, 199 – 207.
[36] Gaussian 16, Revision B.01, M. J. Frisch, G. W. Trucks, H. B. Schlegel, G. E. Scuseria, M. A. Robb, J. R. Cheeseman, G. Scalmani, V. Barone, B. Mennucci, G. A. Petersson, et al., Gaussian, Inc. Wallingford CT, **2016**.
[37] K. B. Wiberg, *Tetrahedron* **1968**, *24*, 1083 – 1096.
[38] A. E. Reed, R. B. Weinstock, F. Weinhold, *J. Chem. Phys.* **1985**, *83*, 735 – 746.
[39] E. D. Glendening, C. R. Landis, F. Weinhold, NBO 6.0. Theoretical Chemistry Institute, University of Wisconsin, Madison, WI, **2013**.
[40] D. Y. Zubarev, A. I. Boldyrev, *Phys. Chem. Chem. Phys.* **2008**, *10*, 5207 – 5217.
[41] D. Y. Zubarev, A. I. Boldyrev, *J. Org. Chem.* **2008**, *73*, 9251 – 9258.
[42] T. A. Keith, TK Gristmill Software, Overland Parks, USA, **2019**.
[43] P. Pyykkö, *J. Phys. Chem. A* **2015**, *119*, 2326 – 2337.
[44] S. Alvarez, *Dalton Trans.* **2013**, *42*, 8617 – 8636.
[45] C. Foroutan-Nejad, *Angew. Chem. Int. Ed.* **2020**, *59*, 20900 – 20903; *Angew. Chem.* **2020**, *132*, 21086 – 21089.
[46] R. Hoffmann, H. Hopf, *Angew. Chem. Int. Ed.* **2008**, *47*, 4474 – 4481; *Angew. Chem.* **2008**, *120*, 4548 – 4556.

Manuscript received: January 20, 2021
Accepted manuscript online: February 1, 2021
Version of record online: March 8, 2021

